Peer-reviewed version available at *Water* **2017**, *9*, 86; doi:10.3390/w9020086

Article

Space-Time Characterization of Rainfall Field in Tuscany

Alessandro Mazza [1,2]

[1] National Research Council, Institute of Biometeorology, Via Gino Caproni 8, Florence 50141, Italy; mazza@lamma.rete.toscana.it; Tel.: +39-55-448-301
[2] LaMMA Consortium, Via Madonna del Piano 10, Sesto Fiorentino 50019, Italy

Abstract: Precipitation during 2001-2016 over the northern and central part of Tuscany was studied in order to characterize the rainfall regime. The dataset consisted of hourly cumulative rainfall series recorded by a network of 801 rain gauges. The territory was divided into 30x30 km square areas, the annual, seasonal and daily Average Cumulative Rainfall (ACR) in all areas was estimated along with its uncertainty. The trend analysis of ACR time series was performed by means of the Mann-Kendall test. Four climatic zones were identified: the north-western was the rainiest, followed by the north-eastern, north-central and south-central. An overall increase in precipitation was identified, more intense in the north-west, and determined mostly by the increase in winter precipitation. On the entire territory, the ACR, number of rainy days, mean precipitation intensity and sum of daily ACR in four intensity groups were evaluated at annual and seasonal scale. The main result was a magnitude of the ACR trend evaluated as 35 mm/year, due mainly to an increase in light and extreme precipitations. This result is in contrast with the decreasing rainfall detected in the past decades.

Keywords: rainfall; rain gauge; kriging, trend detection

1. Introduction

In recent decades there has been a gradual increase in the average temperature of the atmosphere. The global warning has determined a higher water vapor concentration and so an increase in global precipitation [1]. Despite this overall scenario, a decrease in rainfall was found in the Mediterranean area; for example in Italy and Spain the experimental results indicated a reduction in precipitation [2,3]. Along with the decrease in the average rainfall amount there has been a change in rainfall patterns, with extreme precipitation events becoming more frequent [4]; in particular Brunetti [5] and Martinez [6] found similar results for Italy and northern Spain (Catalonia). This behavior was not homogeneous on the Italian territory, being more pronounced in the north [7].

Climate change may cause increased drought and extreme events, therefore the study of the evolution of the rainfall regime is a very important task to construct a hydrological model, prevent flooding and hydraulic risk [8][9]. It is therefore necessary to study rainfall phenomena in different time periods. Evaluation of the rainfall regime for relatively long time periods, annual or seasonal, is essential to study climate change and for hydrological models. Prevention of hydraulic risks needs the assessment of rainfall phenomena for relatively short time periods, daily or hourly. In this perspective, the rainfall amount falling on the territory has to be estimated along with the evaluation of its uncertainty in order to establish the reliability of the results.

In this study the rainfall regime in Tuscany region was analyzed during the years 2001-2016. The instrumentation used was a rain gauge network that provides punctual measurements of the cumulative rainfall. There were only a limited number of rain gauges in the territory, the typical distance between devices was in the order of a few kilometers in more populated areas and more than ten km in hilly areas.

Peer-reviewed version available at Water 2017, 9, 86; doi:10.3390/w9020086

The spatial variability of the cumulative rainfall field implies that for a distance in the order of a few km the values of the correlation coefficient of such an observable is very low [10-12]. Therefore, by means of a rain gauge network with such a low density it was not possible to reconstruct the details of the rainfall field using some spatialization techniques. Given the limitation of the instrumentation an observable was chosen that evaluates the overall rainfall amount on a selected area: the Average Cumulative Rainfall (ACR) i.e. the cumulative rainfall averaged over the area. The spatialization technique chosen to estimate the ACR was Non Parametric Ordinary Block Kriging (NPBOK) [13-18]. This technique allows the best value to be estimated and the standard deviation of the ACR, which is a measure of the uncertainty.

An observable closely related to the ACR is the Rain Volume (RV) i.e. the ACR multiplied by the area; RV can be estimated during the thunderstorms by means of the area time integral method, a technique based on not quantitative rainfall detection [19-20]. Griffith et al [21] used geosynchronous visible or infrared satellite imagery to estimate rainfall over large space and time scales. All these techniques are characterized by lower spatial and temporal resolution.

The estimation of ACR degrades the spatial resolution compared to the punctual cumulative rainfall but it allows the amount of rainfall to be assessed on a selected area. In this context, the Tuscany territory was divided into square areas where the ACR was estimated. The uncertainty of the ACR decreases by increasing the area under consideration, but the increase in the area deteriorates the spatial resolution. A compromise was therefore found for the area size that allows a satisfactory spatial resolution and an acceptable uncertainty of ACR estimates.

The annual, seasonal and daily ACR were estimated for all the areas, the difference in the precipitation amount in different parts of the territory was highlighted. The trend detection of annual and seasonal ACR time series was performed by means of the Mann-Kendall test. The analysis showed a higher rainfall amount in the north-western part of the territory, and an overall increase in precipitation during the period, more pronounced on the Tyrrhenian coast. This rainfall increase occurred mainly in winter. The precipitation increment in Tuscany is contrary to that of previous decades, when a null or negative trend of rainfall was recorded [22,23]. The analysis of daily ACR time series showed an increase in extreme precipitation events, therefore in this case, in agreement with the results obtained for the following years [5,7].

2. Data and Methodology

2.1. Data

The instrumentation used to evaluate the rainfall field was a weather station network that consists of measurement points equipped with rain gauges and other meteorological sensors. The rain gauges measure the cumulative rainfall with the lower accumulation time of one hour. The network is managed by the "Hydrological Service of Tuscany Region" that provides the quality control of the data. The area covered by the network extends over the Tuscany region and neighboring areas of Emilia-Romagna, Lazio and Umbria. Figure 1 reports the rain gauges located in Tuscany in 2014.

Preprints (www.preprints.org) | NOT PEER-REVIEWED | Posted: 31 October 2016 doi:10.20944/preprints201610.0129.v1

Peer-reviewed version available at Water 2017, 9, 86; doi:10.3390/w9020086

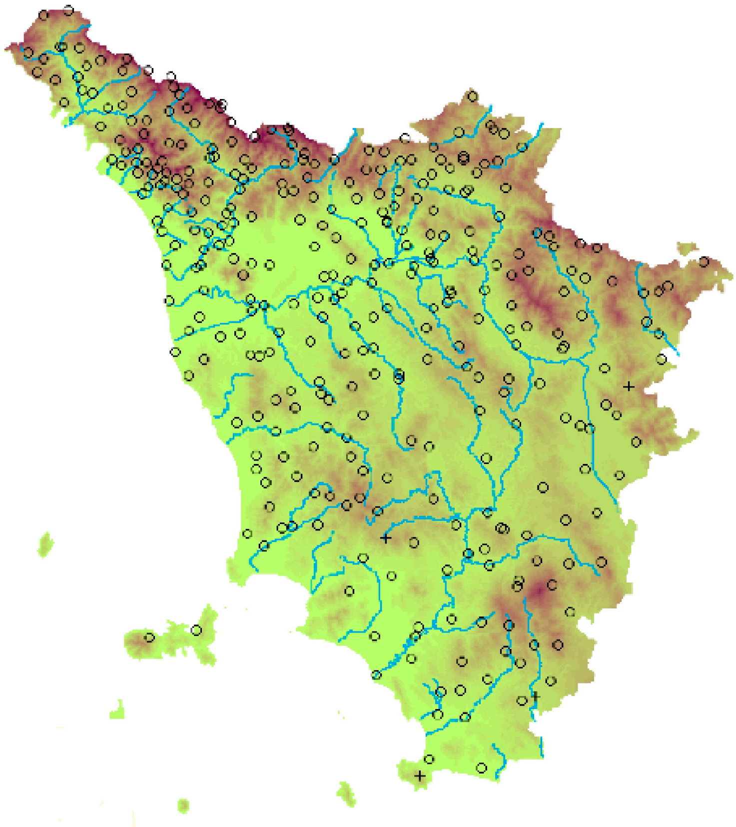

Figure 1. The Tuscany weather station network.

The number of rain gauges increased during the period considered (2001-2016) as new devices were installed: 325 in 2001 and 801 in 2016. The cumulative rainfall for different accumulation times were evaluated for each rain gauge by adding the hourly measurements. The accumulation times considered were: annual (from 1 September to 31 August), seasonal (from 1 September to 30 November in autumn, from 1 December to 28 or 29 February in winter, from 1 March to 31 May in spring and from 1 June to 31 August in summer) and daily.

Only cumulative rainfall measurements of rain gauges that during the accumulation time had recorded more than 90 percent of the hourly measurements were considered. The results obtained were multiplied by the ratio between the number of hours of the accumulation time and the number of hourly measurements recorded in order not to underestimate the result. This procedure eliminates the bias due to the loss of hourly measurements, but introduces an increase in the uncertainty of the cumulative rainfall.

2.2. The NPOBK technique

The complete characterization of the rainfall regime on the territory can be obtained by evaluating the amount of water that falls on an arbitrary area for an arbitrary time period; this can be obtained by means of the observable ACR, which can be expressed in terms of rain rate as:

$$ACR\,(A,T) = \frac{1}{A}\int_A \int_0^T r(x,t)\,dx\,dt = \int_A C(x)\,dx \, , \tag{1}$$

where t is an arbitrary instant of time period T, x an arbitrary point inside area A, r the rain rate evaluated in point x and time t, C(x) the cumulative rainfall in point x.

Determination of the rain rate field for every instant and every point is a necessary and sufficient condition to determine the ACR for any space-time domain. This is obviously impossible given the limitations of the measurements provided by the available instrumentation; the rain gauges perform cumulative rainfall measurements that represent an integral of rain rate,

Peer-reviewed version available at Water 2017, 9, 86; doi:10.3390/w9020086

furthermore they are only installed at a limited number of points. The first limitation implies that 1h is the shortest accumulation time to evaluate the ACR. The second implies that the ACR estimates should be made by means of a spatialization of the measurements. The spatialization technique used was the NPOBK; it is based on the assumption that the cumulative rainfall field C(x) is statistically describable by means of a second order stationary random function [13-18] i.e. the first and second moments are invariant under translations; they are described by means of the following equation:

$$m = E[C(x)]$$
$$F(h) = E[C(x) - m][C(x+h) - m]' \tag{2}$$

where E[] is the mean value operator, m the mean value of cumulative rainfall independent of point x, F(h) the correlation function that depends only on the distance h of the two points as also the isotropy of the field was assumed [13]. The technique produces an interpolation function that gives the best unbiased linear estimate of the ACR (Equation 3) and its variance (σ^2_{ACR}) (Equation 4):

$$ACR(A,T) = \sum_{\alpha=1}^{N} \lambda_\alpha C(x_\alpha), \tag{3}$$

$$\sigma^2_{ACR} = \sum_{\alpha=1}^{n} \lambda_\alpha \gamma_{\alpha V} - \gamma_{VV} - \mu \qquad \gamma_{\alpha V} = \frac{1}{|A|}\int_A \gamma(x_\alpha, x)dx \qquad \gamma_{VV} = \frac{1}{|A|^2}\int_A\int_A \gamma(x,y)dxdy, \tag{4}$$

where $C(x_\alpha)$ is the rain gauge measurement value on the points x_α, A the area, T the accumulation time, γ(x, y) the variogram relative to the pair of points x and y. The parameters λ_α and μ are the solution of the following linear equations system:

$$\sum_{\alpha=1}^{N} \lambda_\alpha \gamma(x_\alpha, x_\beta) - \mu = \gamma_{\beta V} \qquad \beta = 1,\ldots,\mathrm{N} \tag{5}$$

The uncertainty of the ACR estimate was a decreasing function of the number of rain gauges installed within and near the analyzed area, so the size of the area had to be large enough to contain a sufficient number of these in order to perform acceptably accurate estimates. It is worth noting that to estimate ACR only rain gauge measurements placed within or in proximity to area A were used. The use of measurements away from the area decreases the value of the variance very little at the price of a substantial increase of the calculation time required.

The variogram, for the isotropy of the model, is a function that depends only on the distance of the points and it can be evaluated by the following equation:

$$\gamma(h) = \frac{1}{2} Var[C(x) - C(x+h)] = \frac{1}{2}\left[\left\langle (C(x) - C(x+h))^2 \right\rangle - \left\langle (C(x) - C(x+h)) \right\rangle^2\right]. \tag{6}$$

C(x) is second order stationary therefore the second term of the second member is equal to zero (Equation 2). The sample values of the variogram was estimated not parametrically, i.e. without supposing *a priori* the shape of this one, evaluating approximately the second member of Equation 6 by means of the following relationship:

$$\gamma(h) = \frac{1}{2n(h)} \sum_{i=0}^{n(h)} [C(x_i) - C(x_i + h)]^2, \tag{7}$$

where $C(x_i)$ are the cumulative rainfall measurements of the rain gauges installed in point x_i. The sample values of the variogram were determined accurately by considering large values of n(h), therefore using the measurements of rain gauges installed in a large area N. To determine the largest area N where the field was stationary, the variogram was evaluated using measurements of the rain gauges located within increasingly larger areas centered on the same point. When increasing the size of the area a significant increase was observed in the sill evaluation of the variogram, so the field

Preprints (www.preprints.org) | NOT PEER-REVIEWED | Posted: 31 October 2016 doi:10.20944/preprints201610.0129.v1

Peer-reviewed version available at *Water* **2017**, *9*, 86; doi:10.3390/w9020086

cannot be considered stationary. Indeed, the apparent growth of the sill is due to the non-stationarity of the field, so in this case the second term of the second member of Equation 6 is not negligible and therefore Equation 7 does not accurately determine the sample values of the variogram. To avoid negative values of the ACR variance a conditionally negative defined variogram [15-18] was assumed. For this reason, the variogram was determined by fitting the sample values with the following exponential function [18]:

$$\gamma(h)=Q\left(1-\exp\left(-\frac{|h|}{r}\right)\right), \tag{8}$$

where Q and r are the fitting parameters.

The rain rate field was always different for each area and in each time as each rainfall phenomenon has peculiar properties, so the characteristics of the accumulation rainfall field were different for each analyzed case. For this reason, for each ACR estimate the procedure described above was repeated in all cases, first the maximum area was determined where the accumulation rainfall field was stationary, then the variogram was calculated using Equations 7,8.

2.3. ACR estimation

The territory was divided into square areas, the annual, seasonal and daily ACR were evaluated for each area during the period 1 March 2001 – 31 May 2016. The annual and seasonal ACR were estimated by means of the NPOBK technique described in section 2.2. The relative error, defined by $3\sigma_{ACR}$/ACR, was evaluated. Only ACR estimates with relative error lower than 90 percent were considered sufficiently accurate.

The size of the areas had to be large enough to contain a sufficient number of rain gauges in order to perform an acceptably accurate ACR estimate. Conversely, the spatial resolution of accumulation rainfall field is better for small areas. Based on these statements the choice of the size of square areas was 30x30 km^2, which is the best compromise between a good resolution and an acceptable uncertainty of the observable. Only the northern and central part of Tuscany was examined, as the low density of rain gauges installed in the southern part of the region does not allow the ACR to be estimated with sufficient accuracy (Figure 2).

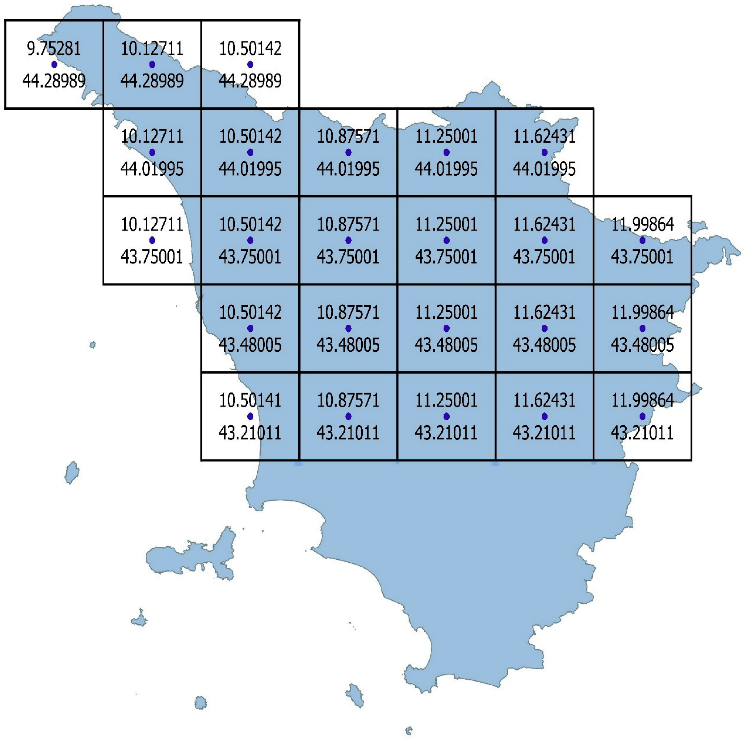

Figure 2. Areas where the ACR was estimated. Latitude and longitude of the centers of the areas are reported.

There were over a hundred thousand daily ACR estimates, a very large number. The algorithm to perform the NPOBK is computationally expensive so it was not possible to estimate the daily ACR in a reasonable amount of time. Alternatively, the daily ACR were evaluated by mediating the cumulative rainfall measurements recorded by rain gauges within the area. This technique, identified by AM, provides less accurate estimates than the NPOBK, and also does not allow the uncertainty to be evaluated. The daily ACR were estimated by both techniques for some special cases, in order to evaluate if the two values were similar. The discrepancy of values was in the order of a few tens of percentage, so the daily AM estimates were considered sufficiently accurate for the aim of this work.

2.4. Characterization of the local rainfall regime

For each area (Figure 2), in order to establish the difference of the typical rainfall amount falling in different zones of Tuscany, the mean of the annual and seasonal ACR over the entire period were considered (ACR_AV). The exact mean and standard deviation of this observable could not be established as the joint probability density function of the relative ACR at different times was unknown. The mean was therefore evaluated approximately averaging the values of the ACR time series.

To establish the rainfall regime evolution, in particular if an increasing or a decreasing in ACR occurred, a trend analysis of annual and seasonal ACR time series was conducted. The statistical test applied was the non parametric Mann Kendall test for autocorrelated data [24,25]. The Z statistic used to perform the trend analysis is a random variable whose probability density function is known and can be approximated to a Gaussian with zero mean and standard deviation equal to 1 for time series with a number of elements greater than or equal to 10. The significance level chosen to reject the null hypothesis, i.e. the absence of a trend, was 0.05, corresponding to $Z>1.96$ (positive trend) or $Z<-1.96$ (negative trend).

The magnitude of the trends was computed using the Theil-Sen estimator (TSA), which is less sensitive to outliers than the least square linear fitting [26,27].

2.5. Characterization of the global rainfall regime

Annual, seasonal and daily ACR evaluated over the entire territory (ACR_TOT) was analyzed in order to study the overall evolution of the rainfall regime. The cumulative rainfall field was not second order stationary as the area was too large, so the NPOBK technique was not applicable. It was therefore chosen to evaluate the mean value of ACR corresponding to the same accumulation time. Once again, the joint probability density function was unknown and so the mean was estimated averaging the ACR values; the standard deviation was not assessed. The following observables were analyzed on annual and seasonal time scales. [27-28]:

ACR_TOT.

Number of rainy days (NRD): the number of days during which daily ACR was greater than 1 millimeter. If the ACR was less than 1 mm, the day was considered not rainy.

Mean intensity of precipitation (MIP): the ACR_TOT divided by NRD.

The sum of daily ACR_TOT falling into these intensity groups: ACR_TOT<10mm (SD0), 10mm<ACR_TOT<25mm (SD10), 25mm<ACR_TOT<40mm (SD25), 40mm<ACR_TOT (SD40).

The time scale will be indicated in subscript to the name of the observable (ann, aut, win, spr, sum indicate the annual and seasonal time scales respectively).

It should be noted that the daily ACR evaluated over relatively large areas never presents the peak of daily cumulative rainfall values observed by some rain gauges, which are essentially punctual measurements. The correlation coefficient of daily cumulative rainfall presents values significantly lower than 1 even for distances of a few km [10-12]. This implies that the peak values may not remain on the whole area. For this reason the threshold value (40 mm) chosen for the last intensity group is significantly lower than the cumulative rainfall measurements of some rain gauges during an extreme event, which may exceed 100 mm.

The trend analysis was performed for all time series and the magnitude of the trends was computed.

3. Results

3.1. Estimation of rainfall amount

The annual and seasonal ACR were estimated for each area (Figure 2) by means of the NPOBK technique during the considered period. Some examples are shown in Table 1 (for some areas and all years and seasons) and in Figures 3-4 (for all areas and some years and seasons). The typical values of the relative error were some tens of percentage points; in all cases it was lower than 75 percent. The density of rain gauges was not homogeneous, it was generally greater near the main cities and in the most populated areas in general (Figure 1), therefore the relative error decreases accordingly. New rain gauges were installed during the considered period so in some areas the uncertainty was lower when evaluated more recently. For some seasons and some areas it was not possible to estimate the ACR since the measurements acquired by rain gauges were less than 90 percent of the total.

It should be noted that for each year the sum of seasonal ACR estimates is not exactly equal to the annual one. This discrepancy is due to two distinct causes. First, the data quality control sometimes excluded the measurements of some rain gauges; the rain gauge measurements excluded by the annual estimates may differ from the seasonal ones. Therefore, the set of data in the interpolation equations (Equation 2) to estimate annual and seasonal ACR were different. Second, the annual and seasonal cumulative rainfall fields and thus the shape of the related variograms did not coincide, so the coefficients of the NPBOK linear systems (Equation 5) related to same rain gauges were different.

Preprints (www.preprints.org) | NOT PEER-REVIEWED | Posted: 31 October 2016 doi:10.20944/preprints201610.0129.v1

Peer-reviewed version available at *Water* **2017**, *9*, 86; doi:10.3390/w9020086

Table 1. Examples of annual and seasonal ACR (mm) and their standard deviations and relative errors. M denotes missing values.

lat: 43.480053 lon: 11.250000															
YEAR	ANNUAL			AUTUMN			WINTER			SPRING			SUMMER		
	ACR	σ	ERR	ACR	σ	ERR	ACR	σ	ERR	ACR	σ	ERR	ACR	σ	ERR
2001-2002	795	99	0.38	229	29	0.38	117	17	0.43	197	25	0.38	172	43	0.75
2002-2003	780	80	0.31	290	30	0.31	238	24	0.31	158	16	0.31	104	26	0.75
2003-2004	870	89	0.31	278	28	0.31	238	24	0.31	227	23	0.31	208	52	0.75
2004-2005	798	89	0.34	143	36	0.75	222	25	0.34	158	18	0.34	226	57	0.75
2005-2006	983	110	0.34	513	57	0.34	220	25	0.34	M	M	M	100	11	0.34
2006-2007	842	86	0.31	240	18	0.23	189	14	0.22	200	13	0.19	78	9	0.34
2007-2008	681	51	0.23	135	11	0.25	188	14	0.23	224	16	0.22	109	11	0.31
2008-2009	931	95	0.31	324	23	0.22	272	17	0.19	221	14	0.19	139	14	0.31
2009-2010	982	61	0.19	200	13	0.19	365	23	0.19	265	15	0.17	96	10	0.31
2010-2011	937	60	0.19	443	30	0.20	230	15	0.19	123	8	0.19	138	14	0.31
2011-2012	541	36	0.20	127	8	0.20	114	8	0.21	224	15	0.20	64	6	0.28
2012-2013	1155	83	0.22	446	31	0.21	261	19	0.22	309	21	0.20	136	34	0.75
2013-2014	1266	95	0.23	418	29	0.21	330	24	0.22	170	13	0.23	233	41	0.53
2014-2015	824	51	0.19	316	19	0.18	203	12	0.18	176	10	0.18	246	27	0.34
lat: 44.019947 lon: 10.875702															
YEAR	ANNUAL			AUTUMN			WINTER			SPRING			SUMMER		
	ACR	σ	ERR	ACR	σ	ERR	ACR	σ	ERR	ACR	σ	ERR	ACR	S	ERR
2001-2002	1375	243	0.53	386	97	0.75	284	35	0.38	324	21	0.19	359	24	0.20
2002-2003	1434	96	0.20	750	48	0.19	408	27	0.20	194	13	0.21	63	5	0.22
2003-2004	1940	130	0.20	701	47	0.20	617	45	0.22	464	31	0.20	171	11	0.19
2004-2005	1036	116	0.34	M	M	M	251	17	0.20	291	19	0.19	194	20	0.31
2005-2006	1459	94	0.19	509	33	0.19	490	33	0.20	M	M	M	199	11	0.17
2006-2007	1328	83	0.19	364	21	0.17	504	29	0.17	251	14	0.16	159	10	0.18
2007-2008	1231	71	0.17	341	20	0.17	353	20	0.17	427	23	0.16	105	6	0.16
2008-2009	1843	109	0.18	677	37	0.16	700	37	0.16	392	21	0.16	111	6	0.15
2009-2010	1906	97	0.15	453	23	0.15	786	39	0.15	361	18	0.15	317	16	0.15
2010-2011	1744	89	0.15	740	38	0.15	575	29	0.15	233	11	0.15	210	10	0.15
2011-2012	1162	59	0.15	384	20	0.15	287	15	0.16	424	21	0.15	80	4	0.15
2012-2013	2193	112	0.15	744	37	0.15	570	29	0.15	815	40	0.15	140	7	0.15
2013-2014	2241	117	0.16	599	31	0.15	1057	54	0.15	290	15	0.16	300	15	0.15
2014-2015	1478	75	0.15	643	33	0.15	374	19	0.15	325	17	0.15	138	7	0.15

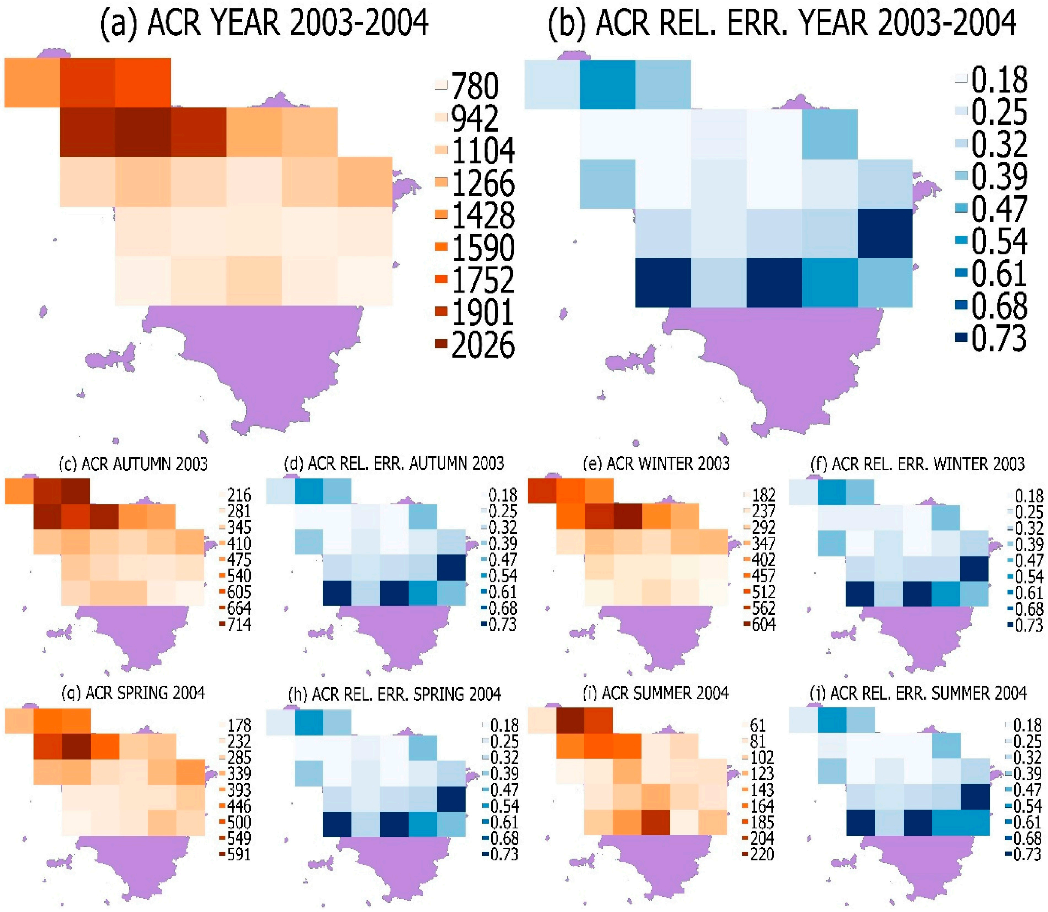

Figure 3. Annual (a) and seasonal (c), (e), (g), (i) ACR (mm) and their relative errors (b), (d), (f), (h), (j), for all areas, year: 2003-2004.

Preprints (www.preprints.org) | NOT PEER-REVIEWED | Posted: 31 October 2016 doi:10.20944/preprints201610.0129.v1

Peer-reviewed version available at Water 2017, 9, 86; doi:10.3390/w9020086

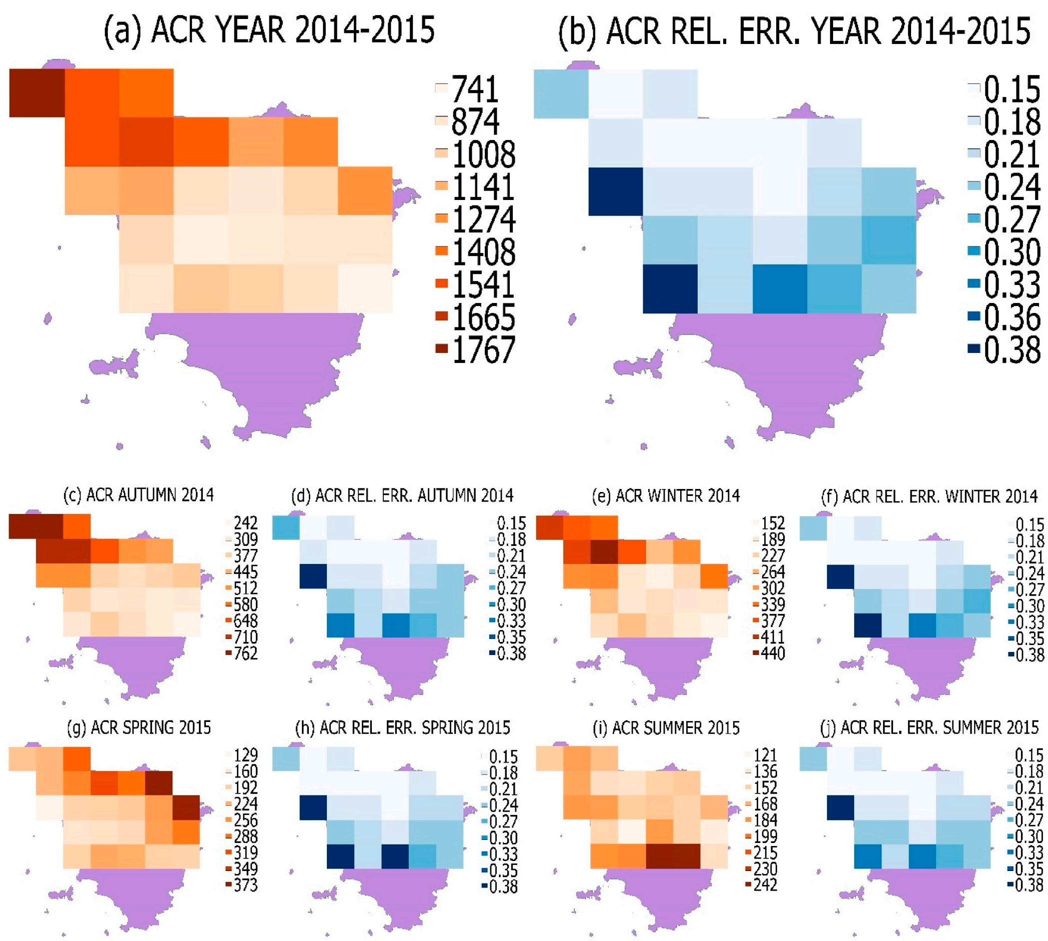

Figure 4. Annual (a) and seasonal (c), (e), (g), (i) ACR (mm) and their relative errors (b), (d), (f), (h), (j), for all areas, year: 2014-2015.

The daily ACR were estimated by the AM technique. Table 2 reports examples of estimates obtained by means of the NPBOK and AM techniques. The results show a discrepancy in the order of some tens of percentage points, which is sufficiently accurate.

Table 2. Comparison of daily ACR estimates obtained by means of AM and NPOBK techniques.

Lat	Lon	Year_Month_Day	ACR AM	ACR NPBOK
43.75	10.13	2001_11_11	4.4	5.2
44.02	10.88	2003_10_07	0.8	0.5
44.02	10.13	2004_10_29	44.1	37.0
44.29	9.75	2006_03_22	12.2	8.9
44.20	10.13	2008_02_29	1.2	1.9
43.75	12.00	2001_07_24	7.5	11.0
43.21	11.25	2013_10_05	17.1	18.7

3.2. The local rainfall regime

The average of annual and seasonal ACR values of each area was calculated; the results are reported in Table 3 and Figure 5. The annual values of ACR_AV highlight different rainfall regimes for different areas. In the central-southern areas (centered at lat. 43.21 and 43.48) ACR_AV were between 800 and 900 mm, in the central-northern areas (centered at lat. 43.75) they were about 1000

Preprints (www.preprints.org) | NOT PEER-REVIEWED | Posted: 31 October 2016 doi:10.20944/preprints201610.0129.v1

Peer-reviewed version available at Water 2017, 9, 86; doi:10.3390/w9020086

mm. In north-western areas (centered at lat. 44.01, 44.28 and lon. 10.12, 10.87) ACR_AV were about 1600 mm, in north-eastern areas (lat. 44.01, lon. 11.25, 11.62) 1100mm.

In spring, the ACR_AV values in the central-southern areas were about 210 mm. In central-northern areas a gradient in the east-west direction was observed, in the east the ACR values were about 200 mm, while in the west 280 mm. In north-western areas they were about 350 mm, while in north-eastern areas 300 mm. In the summer, the ACR_AV values in central-southern and central-northern areas were about 130 mm, in northern areas 200 mm**.** In autumn, in central-southern areas a gradient in the east-west direction was observed, in the west the ACR values were about 350 mm, in the east 250 mm. In central-northern and northern areas values were about 350 mm and 500 mm respectively. In the winter, the ACR values in central-southern areas were about 250 mm, in central-northern areas about 300 mm and 500 mm in northern areas.

Based on these results it may be noted that the annual volume of rainfall decreases moving in the north-south direction; furthermore, the north-western part of the territory was rainier than the north-east. The rainfall regime, on a seasonal basis, reproduces the same behavior, if a region is more rainy annually the same behavior occurs for all seasons.

The trend analysis was performed for the time series of annual and seasonal averaged ACR_AV (Table 3, Figure 5). For almost all cases, the value of the Z statistic of the Mann-Kendall test was positive, which is a clue of a positive trend of the observable. The Z value of many time series was lower than 1.96, the value of the threshold chosen to reject the null hypothesis, therefore it is not possible to state with sufficient confidence the presence of a positive trend in many of the areas considered.

The magnitude of trends of annual ACR were higher in the north-western coastal area, in general the gradient of the trend magnitude was directed towards the north-west; in other words there is a trend increase by moving in the western and northern directions. The typical trend magnitude was some tens of mm/year. In autumn, winter and summer the trend analysis highlights similar behavior to the annual one, in spring the magnitude of the trend was overall homogeneous.

Preprints (www.preprints.org) | NOT PEER-REVIEWED | Posted: 31 October 2016 doi:10.20944/preprints201610.0129.v1

Peer-reviewed version available at Water 2017, 9, 86; doi:10.3390/w9020086

Table 3. Annual and seasonal ACR_AV estimates, values of Z statistic and magnitudes of the trend. The Z values > 1.96 are reported in bold.

		ANNUAL			AUTUMN			WINTER			SPRING			SUMMER		
Lat	Lon	ACR	Z	T	ACR	Z	T	ACR	Z	T	ACR	Z	T	ACR	Z	T
43.21	10.50	914	1.17	23.1	335	-0.48	-3.6	269	1.89	7.9	202	-0.21	-1.8	104	0.62	5.2
43.21	10.88	955	**3.09**	34.3	350	0.06	-0.1	284	**3.03**	9.5	210	0.99	3.5	136	0.44	2.6
43.21	11.25	870	0.95	-0.7	329	-0.22	-1.8	249	1.31	7.0	199	0.43	0.8	146	0.33	2.5
43.21	11.62	827	**5.28**	20.9	273	0.44	1.1	229	0.74	3.0	196	0.99	4.7	130	1.31	7.6
43.21	12.00	730	**2.01**	13.3	235	0.22	0.6	200	0.90	3.5	180	1.48	4.3	129	-0.33	-1.4
43.48	10.50	910	**3.02**	28.1	343	-0.52	-2.5	268	**4.70**	10.7	205	0.59	1.8	109	0.55	1.6
43.48	10.88	824	1.64	23.3	289	0.11	1.5	235	**2.24**	8.4	203	0.59	2.4	113	0.55	2.6
43.48	11.25	885	1.42	19.6	290	1.12	2.2	234	0.89	6.3	213	0.40	1.6	139	0.66	3.4
43.48	11.62	838	**2.31**	15.8	293	-0.44	-1.6	236	1.90	6.0	215	1.09	6.6	123	0.99	1.4
43.48	12.00	852	0.31	3.4	288	-0.11	-2.0	239	1.82	6.8	222	0.43	2.2	124	1.40	3.1
43.75	10.13	956	1.75	30.2	352	-0.32	0.3	279	**2.67**	16.6	203	-0.44	-1.9	123	0.00	1.3
43.75	10.50	1075	1.75	40.6	380	0.32	2.0	339	**4.22**	19.6	242	0.69	3.3	135	1.31	3.2
43.75	10.88	896	1.86	37.8	292	0.55	3.2	270	**2.35**	9.3	210	0.69	2.9	133	0.55	3.2
43.75	11.25	841	2.08	19.1	286	0.10	1.3	242	1.39	9.5	201	0.30	2.6	132	1.73	5.4
43.75	11.62	1079	**2.01**	11.2	351	0.10	1.0	318	1.66	7.0	268	0.20	1.1	148	0.89	4.3
43.75	12.00	1264	**2.87**	35.3	402	0.44	3.6	371	**8.50**	9.3	317	0.30	2.1	166	0.66	3.2
44.02	10.13	1652	1.40	60.4	565	0.33	7.1	523	**3.39**	24.3	354	0.58	1.9	192	0.88	3.3
44.02	10.50	1777	1.65	52.1	614	0.18	3.0	580	**1.98**	28.4	383	0.66	4.8	202	0.00	0.2
44.02	10.88	1598	1.31	44.2	557	0.11	2.0	533	1.68	24.7	378	0.00	0.1	182	-0.22	-3.0
44.02	11.25	1156	1.64	31.8	383	0.10	0.4	371	1.58	14.8	282	0.10	0.4	133	0.79	5.4
44.02	11.62	1113	1.31	29.6	378	0.22	2.8	313	1.85	5.0	301	1.68	6.5	146	0.95	3.7
44.29	9.75	1588	**3.50**	104.6	554	2.47	22.2	521	1.78	26.5	355	0.30	2.3	199	0.88	5.0
44.29	10.13	1792	**1.99**	70.8	608	0.43	8.7	522	1.31	19.7	369	0.33	4.2	205	0.34	3.9
44.29	10.50	1517	**2.12**	40.0	525	-0.06	-0.4	434	1.64	18.9	345	0.55	3.4	195	-0.18	-2.0

Preprints (www.preprints.org) | NOT PEER-REVIEWED | Posted: 31 October 2016 doi:10.20944/preprints201610.0129.v1

Peer-reviewed version available at Water 2017, 9, 86; doi:10.3390/w9020086

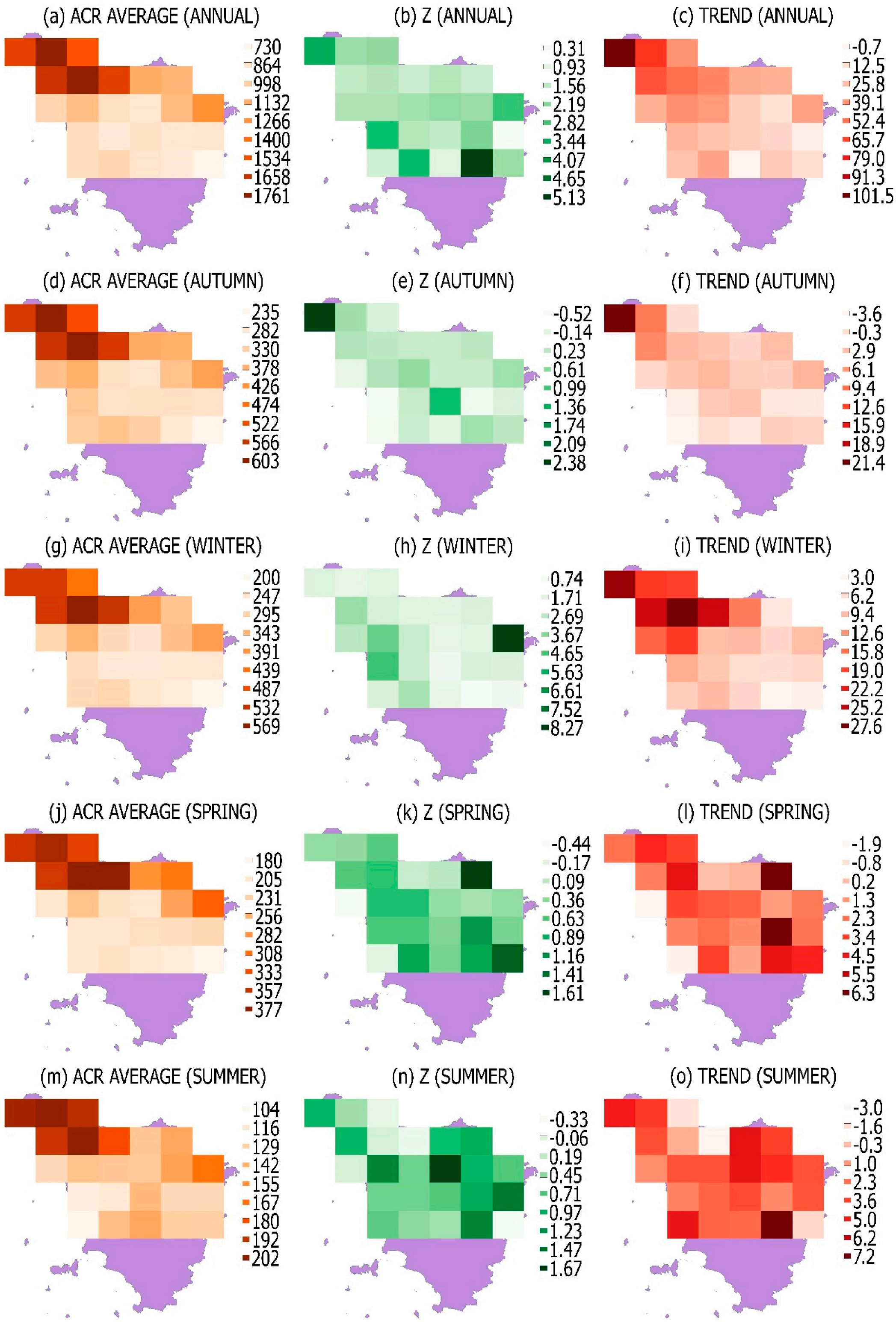

Figure 5. Annual and seasonal ACR_AV estimates (a), (d), (g), (j), (m), values of Z statistic (b), (e), (h), (k), (n), and magnitudes of the trend (c), (f), (i), (l), (o).

3.3. The rainfall regime onthe whole area.

The annual and seasonal values of ACR_TOT, NRD, MIP, SD0, SD10, SD25, SD40 were evaluated (Figures 6-7). The Mann-Kendall test was performed for all time series (Table 4).

ACR_TOT_{ann} highlights an increase in precipitation, the value of the Z statistic equal to 1.86 was very close to the threshold value, suggesting the presence of a growing trend. The trend magnitude

Preprints (www.preprints.org) | NOT PEER-REVIEWED | Posted: 31 October 2016 doi:10.20944/preprints201610.0129.v1

Peer-reviewed version available at *Water* **2017**, *9*, 86; doi:10.3390/w9020086

of 35.4 mm/year indicates a significant increase in the rainfall amount. The Z values of ACR_TOT_{aut}, ACR_TOT_{win}, ACR_TOT_{spr}, ACR_TOT_{sum} show an increase in precipitation only in the winter.

The trend analysis of the NRD_{ann} time series does not clearly highlight an increase in this observable. However, the Z values of seasonal time series show that a positive trend was detected only in the winter.

The Z value of MIP_{ann} was 1.86, also in this case the presence of a positive trend is very likely. The analysis of the Z statistic of the seasonal time series did not show an increase in this observable; although the Z value of MIP_{win} suggests the possible presence of a positive trend in winter.

The study of these observables highlights that one of the causes of the increase in annual precipitation was the growth of MIP_{ann}. The Mann-Kendall test of NRD_{ann} does not clearly show a positive trend, although the Z value might suggest it; therefore it cannot be excluded that this phenomenon could also have caused the increase in annual rainfall. For all the considered time series the positive trend was always attributable to a change of the rainfall regime in winter, a clear growth of the observables was not highlighted in the other seasons.

The trend analysis of $SD0_{ann}$ shows a positive trend, the value of the Z statistic was 2.36. The magnitude of trend equal to 13.3 mm/year was very high, so the rainfall amount caused by low-intensity phenomena has increased a lot during the considered period. $SD10_{ann}$ and $SD25_{ann}$ did not show any positive trend, so the rainfall amount due to medium intensity phenomena can be considered stationary. The value of the Z statistic of $SD40_{ann}$ was 2.58, so the presence of a positive trend was established. The magnitude of the trend equal to 10.5 mm/year was very high; it shows a significant increase in the contribution of extreme events to the rainfall amount.

The analysis of seasonal time series shows that the rainfall regime in autumn, winter and summer was similar to the annual one, there was an increase in rainfall amount for the light and extreme precipitations and substantially stable for the intermediate ones. In the spring no trend was observed in any of the intensity groups.

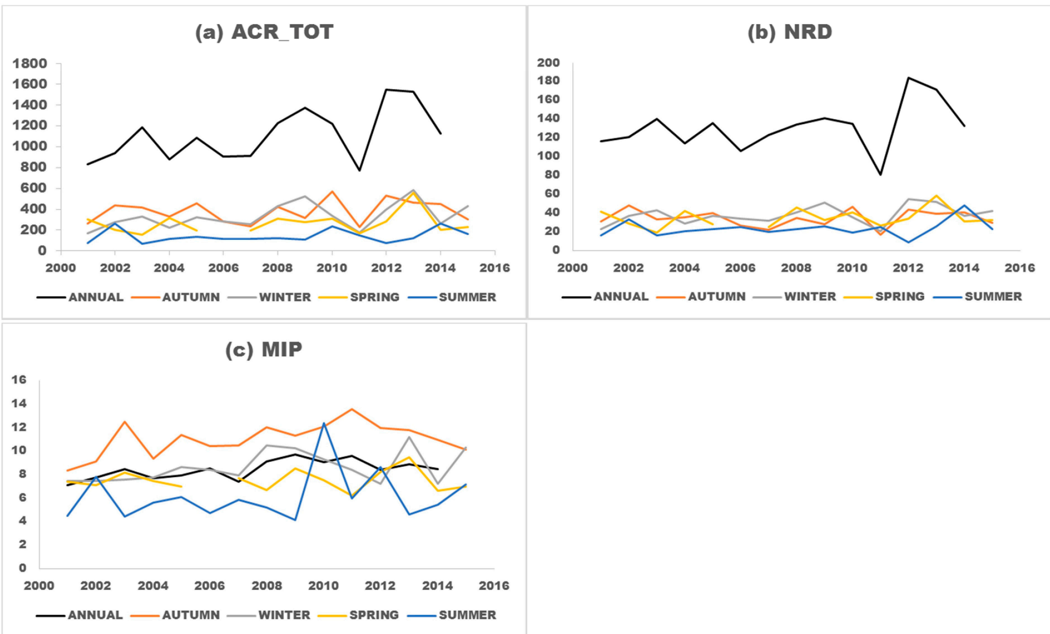

Figure 6. Annual and seasonal time series of: ACR_TOT (a), NRD (b) and MIP (c).

Preprints (www.preprints.org) | NOT PEER-REVIEWED | Posted: 31 October 2016 doi:10.20944/preprints201610.0129.v1

Peer-reviewed version available at Water 2017, 9, 86; doi:10.3390/w9020086

Figure 7. Annual and seasonal time series of: SD0 (a), SD10 (b), SD25 (c) and SD40 (d).

Table 4. Values of Z statistic and trend magnitudes of annual and seasonal observables.

	ANNUAL		AUTUMN		WINTER		SPRING		SUMMER	
	Z	T	Z	T	Z	T	Z	T	Z	T
ACR_TOT	1.86	35.4	0.49	2.9	**3.57**	14.8	0.20	1.1	1.48	3.9
NRD	1.20	2.2	0.00	-0.1	**3.37**	1.1	0.69	0.4	1.14	0.5
MIP	1.86	0.1	1.29	0.2	1.58	0.1	0.00	0.0	0.79	0.1
SD0	**2.36**	13.3	1.68	3.3	1.78	3.1	0.40	0.6	**4.16**	2.7
SD10	0.71	4.3	-0.79	-1.6	1.48	6.5	0.10	0.5	0.40	1.7
SD25	0.88	7.6	0.30	0.5	0.94	2.8	0.10	0.0	-1.14	0.0
SD40	**2.58**	10.5	1.51	0.2	**3.96**	2.689	0.68	0.0	1.50	0.0

5. Discussion and Conclusion

The estimate of rainfall amount is fundamental to evaluate the rainfall regime on the territory. The observable introduced to perform this task was the ACR [13,14] evaluated on some square areas composing the studied territory. Along with the best value of the observable it is very important to quantitatively evaluate the uncertainty to establish the validity of the results. The annual and seasonal ACR was therefore estimated along with its uncertainty, spatializing the measurements of a rain gauge network by means of the NPOBK technique [13-18]. The daily measurements were evaluated without an assessment of the error.

The uncertainty was due mainly to the limited density of rain gauges on the territory; indeed the standard deviation of the ACR estimate depends essentially on the number of rain gauges in the area. In this context, a compromise was reached about the size of the square areas (30x30 km^2) that allows a satisfactory spatial resolution and an acceptable uncertainty. Only the northern and central part of Tuscany was studied as the low density of rain gauges in the south does not allow acceptable estimates to be obtained. The period considered was: 1 March 2001- 31 May 2016.

The results can be summarized as follows:

the territory can be divided in four areas distinguished by the ACR_AV values during the considered period. The north-western area is the rainiest (ACR_AV about 1600 mm) and experienced the higher increment in precipitation. The north-eastern area (ACR_AV about 1200 mm), central area (ACR_AV about 1000 mm) and southern-central area (ACR_AV about 800 mm) had the most limited increment in precipitation. For all areas the precipitation in autumn and winter was more abundant than in spring; summer precipitation was the least abundant.

The ACR_TOT time series showed a very strong increment in precipitation; the increase was assessed as 35 mm/year and was mainly due to winter rainfall. This was caused by the positive trend in MIP and probably also in NRD. The ACR_TOT positive trend was not homogenous on the territory but the magnitude of the trend was higher in the north-western area. Analysis of the distribution of daily precipitation shows an increase in the contribution of low and extreme intensity phenomena, while the contribution of medium intensity phenomena can be considered stationary.

The increase in rainfall that occurred during the considered period is in contrast with the overall trend of the last decades. Bartolini et al. [23] showed a tendency to a decrease in rainfall during the period 1948-2009 in two distinct sites in Tuscany, while Fatichi et al.[22] during the period 1916-2003 showed an absence of any trends in precipitation amount or intensity of extreme events.

The results of this paper are only apparently surprising. Within a generally decreasing rainfall trend a period of increase in precipitation may occur without affecting the overall trend. For example, Romano et al. [28] showed an overall decreasing trend in annual precipitation in the Tiber river basin, an area close to Tuscany. The details of the behavior of the rainfall time series showed a succession of dry and wet periods when the rainfall amount increased.

The values of SD40 observable are increased, so extreme rainfall phenomena have become more frequent. This result is in agreement with Crisci et al. [29] who reported an increase of extreme events in Tuscany during the period 1973-1994, while Fatichi et al. [22] did not detect any trend on the basis of a longer time series. The increase in extreme precipitation aggravates the risk of flooding, in this context the monitoring of these phenomena, also with the technique described in this paper, becomes essential.

In the future the ACR estimates will be improved by means of the measurements of radar operating on the territory. The radar can measure the average rain rate on 1x1 km square pixels, so can improve the spatial resolution of ACR estimates. The radar sweeps all Tuscany, so the measurements will allow the rainfall regime to be studied over the whole region.

Acknowledgments: The Tuscany region meteorological network managed by the Hydrological Service of Tuscany provided rain gauge data.

References

1. Trenberth, K. E.; Dai, A.; Rasmussen, R. M.; Parsons, D. B. The changing character of precipitation. *B. Am. Meteorol. Soc.* **2003**, *84*, 1205–1217, http://dx.doi.org/10.1175/BAMS-84-9-1205.
2. Brunetti, M.; Maugeri, M.; Monti, F.; Nanni, T. Temperature and precipitation variability in Italy in the last two centuries from homogenised instrumental time series. *Int. J. Climatol.* **2006**, *26*, 345–381, http://dx.doi.org/10.1002/joc.1251.
3. Romero, R.; Guijarro, J. A.; Ramis, C.; Alonso, S. A 30-year (1964–1993) daily rainfall data base for the Spanish Mediterranean regions: first exploratory study. *Int. J. Climatol.* **1998**, *18*, 541–560, http://dx.doi.org/10.1002/(SICI)1097-0088(199804)18:5<541::AID-JOC270>3.3.CO;2-E.
4. Alpert, P. The paradoxical increase of Mediterranean extreme daily rainfall in spite of decrease in total values. *Geophys. Res. Lett.* **2002**, *29*, 31.1-31.4, http://dx.doi.org/10.1029/2001GL013554
5. Brunetti, M.; Maugeri, M.; Nanni, T. Changes in total precipitation. rainy days and extreme events in northeastern Italy. *Int. J. Climatol.* **2001**, *21*, 861–871, http://dx.doi.org/10.1002/joc.660.
6. Martínez, M. D.; Lana, X.; Burgueño, A.; Serra, C. Spatial and temporal daily rainfall regime in Catalonia (NE Spain) derived from four precipitation indices. years 1950–2000. *Int. J. Climatol.* **2007**, *27*, 123–138, http://dx.doi.org/10.1002/joc.1369.
7. Brunetti, M.; Colacino, M.; Maugeri, M.; Nanni, T. Trends in the daily intensity of precipitation in Italy from 1951 to 1996. *Int. J. Climatol.* **2001**, *21*, 299–316, http://dx.doi.org/10.1002/joc.613.
8. Jang, J.H. An advanced method to apply multiple rainfall thresholds for urban flood warnings. *Water* **2015**, *7*, 6056–6078, http://dx.doi.org/10.3390/w7116056.

9. Notaro, V.; Liuzzo, L.; Freni, G.; La Loggia, G. Uncertainty analysis in the evaluation of extreme rainfall trends and its implications on urban drainage system design. *Water* **2015**, *7*, 6931–6945, http://dx.doi.org/10.3390/w7126667.
10. Pedersen, L.; Jensen, N. E.; Christensen, L. E.; Madsen, H. Quantification of the spatial variability of rainfall based on a dense network of rain gauges. *Atmos. Res.* **2010**, *95*, 441–454, http://dx.doi.org/10.1016/j.atmosres.2009.11.007.
11. Mandapaka, P. V.; Krajewski, W. F.; Ciach, G. J.; Villarini, G.; Smith, J. A. Estimation of radar-rainfall error spatial correlation. *Adv. Water Resour.* **2009**, *32*, 1020–1030, http://dx.doi.org/10.1016/j.advwatres.2008.08.014.
12. Ciach, G. J.; Krajewski, W. F. On the estimation of radar rainfall error variance. *Adv. Water Resour.* **1999**, *22*, 585–595, http://dx.doi.org/10.1016/S0309-1708(98)00043-8.
13. Mazza, A.; Antonini, A.; Melani, S.; Ortolani, A. Recalibration of cumulative rainfall estimates by weather radar over a large area. *J. Appl. Remote Sens.* **2015**, *9*, 95993.1-95993.21, http://dx.doi.org/10.1117/1.JRS.9.095993.
14. Mazza, A.; Antonini, A.; Melani, S.; Ortolani, A. Estimates of cumulative rainfall over a large area by weather radar. In Remote Sensing of Clouds and the Atmosphere XIX; and Optics in Atmospheric Propagation and Adaptive Systems XVII. Proceedings of SPIE Remote Sensing and Security, Amsterdam, Netherlands, 22-25 September 2014; Comerón, A., Kassianov, E. I., Schäfer, K., Picard, R. H., Stein, K., Gonglewski, J. D., p. 92420V, http://dx.doi.org/10.1117/12.2066492.
15. Chiles, J. P.; Delfiner, P. B. Structural analysis. In *Geostatistics: Modeling Spatial Uncertainty*, 2nd ed.; Balding, D. J., Cressie, N. A., Eds.; John Wiley & Sons: Hoboken, New Jersey, 2012; pp. 28–146.
16. Chiles, J. P.; Delfiner, P. B. Kriging. In *Geostatistics: Modeling Spatial Uncertainty*, 2nd ed.; Balding, D. J., Cressie, N. A., Eds.; John Wiley & Sons: Hoboken, New Jersey, 2012; pp. 147–237.
17. Wackemagel, H. Geostatistics. In *Multivariate. Geostatistics An Introduction with Applications*, 3rd ed.; Eds.; Springer-Verlag: Berlin, Germany, 2003; pp. 35–120.
18. Armstrong, M. The theory of kriging. In *Basic Linear Geostatistics*, 1st ed.; Eds.; Springer-Verlag: Berlin, Germany, 1998; pp. 83–102.
19. Doneaud, A.; Ionescu-Niscov, S.; Priegnitz, D. L.; Smith, P. L. The area-time integral as an indicator for convective rain volumes. *J. Clim. Appl. Meteorol.* **1984**, *23*, 555–561, http://dx.doi.org/10.1175/1520-0450(1984)023<0555:TATIAA>2.0.CO;2.
20. Doneaud, A. A.; Smith, P. L.; Dennis, A. S.; Sengupta, S. A simple method for estimating convective rain volume over an area. *Water Resour. Res.* **1981,** *17*, 1676–1682, http://dx.doi.org/10.1029/WR017i006p01676.
21. Griffith, C. G.; Woodley, W. L.; Grube, P. G.; Martin, D. W.; Stout, J.; Sikdar, D. N. Rain estimation from geosynchronous satellite imagery—visible and infrared studies. *Mon. Weather Rev.* **1978**, *106*, 1153–1171, http://dx.doi.org/10.1175/1520-0493(1978)106<1153:REFGSI>2.0.CO;2.
22. Fatichi, S.; Caporali, E. A comprehensive analysis of changes in precipitation regime in Tuscany. *Int. J. Climatol.* **2009**, *29*, 1883–1893, http://dx.doi.org/10.1002/joc.1921.
23. Bartolini, G.; Grifoni, D.; Torrigiani, T.; Vallorani, R.; Meneguzzo, F.; Gozzini, B. Precipitation changes from two long-term hourly datasets in Tuscany, Italy. *Int. J. Climatol.* **2014**, *34*, 3977–3985, http://dx.doi.org/10.1002/joc.3956.
24. Hamed, K. H.; Ramachandra Rao, A. A modified Mann-Kendall trend test for autocorrelated data. *J. Hydrol.* **1998**, *204*, 182-196, http://dx.doi.org/10.1016/S0022-1694(97)00125-X.
25. Hipel, K. W.; McLeod, A. I. Non parametric test for trend detection. In *Time Series Modelling of Water Resources and Environmental Systems*, 1st ed.; Eds.; Elsevier: Amsterdam, Netherlands, 1994; pp. 853–938.
26. Sen, P. K. Estimates of the regression coefficient based on Kendall's Tau. *J. Am. Stat. Assoc.* **1968**, *63*, 1379-1389, http://dx.doi.org/10.2307/2285891.
27. Qu, B.; Lv, A.; Jia, S.; Zhu, W. Daily precipitation changes over large river basins in China. 1960–2013. *Water* **2016**, *8*, 185, http://dx.doi.org/10.3390/w8050185.
28. Romano, E.; Preziosi, E. Precipitation pattern analysis in the Tiber River basin (central Italy) using standardized indices. *Int. J. Climatol.* **2013**, *33*, 1781–1792, http://dx.doi.org/10.1002/joc.3549.

 doi:10.20944/preprints201610.0129.v1

Peer-reviewed version available at *Water* **2017**, *9*, 86; doi:10.3390/w9020086

29. Crisci, A.; Gozzini, B.; Meneguzzo, F.; Pagliara, S.; Maracchi, G. Extreme rainfall in a changing climate: regional analysis and hydrological implications in Tuscany. *Hydrol. Process.* **2002**, *16*, 1261–1274, http://dx.doi.org/10.1002/hyp.1061.